v1: 1 January 2024

Research Article

Propagation of Electromagnetic Waves Through Complex Space for Astronomical Redshift Investigation

Peer-approved: 1 January 2024

Qeios, Vol. 6 (2024)
ISSN: 2632-3834

Peter Chen[1]

1. Former School of Mechanical and Manufacturing Engineering, University of New South Wales, Australia

Space has a complex structure, and investigations of any electromagnetic wave transmission theory need to consider the inhomogeneous and anisotropic nature. We have selected two cases for our investigations: regions of pulse energy changes and gravitational deflection. Numerical methods have been developed, and examples are given to show that these conditions do have their localized effects. However, since the total length of those regions is insignificant in comparison with the total transmission distance involved, their inclusion does not significantly alter the linear relationship between wavelength change and distance travelled. The possible exception is the case of gravitational deflection when the waves have passed through densely populated regions of space. Our findings could be of interest to the current debate on Hubble tension.

Correspondence: papers@team.qeios.com — Qeios will forward to the authors

1. Introduction

In recent years, we have published three papers [1][2] [3] about how the nonlinear Schrodinger equation (NSE) could be used to find out wavelength changes in electromagnetic waves propagating through space. As the only direct and easily measurable physical quantity from space, electromagnetic waves have been widely used to study the universe. For example, redshift, the lengthening of the wavelength in starlight, has been used to determine the distance of a star, and the size and origin of the universe. To be sure that those applications are reliable, it is important to understand the physics involved in redshift. Up to recent years, there have been realizations that we still need new physics to explain this phenomenon [4]. Although the physics behind NSE is not new, we have shown that redshift could be predicted. In this paper, we report our further investigation and provide additional evidence to support the wave propagation theory.

Solving NSE numerically, we have generated waveforms specifically for bright [1], dark [2] and anti-dark [3] solitons. These are respectively white, dark, and grey spectral lines used by astronomers to determine the extent of wavelength changes in starlight coming from space. We have shown that those solitons can propagate stably over long distances through space. But the previous model used involves only two system parameters: namely, the dispersion coefficient and one for the nonlinear focusing term. In reality, space is a much more complex medium with many regions having localized unique features. In this paper, we shall include two extra features into our model: (i) pulse energy changes due to prevalent atmospheric conditions, and (ii) gravitational deflection of the light path.

In propagating through some sections of a vast distance in space, electromagnetic waves could encounter

 doi.org/10.32388/XFMF84.2

atmospheric conditions that impart or absorb energy from the waves. The two cases of pulse energy changes we consider are (i) elements present in the atmosphere that emit or absorb pulse energy of similar frequency, resulting in the increase or decrease of pulse amplitude, and (ii) the CW background that causes pulse energy to change. To account for these additional parameters, NSE has been modified accordingly.

According to General Relativity Theory, a travelling light path would be deflected near the proximity of a vast mass. Depending on the system involved, the full mathematical analysis is rather complicated. We shall use an approximate solution [4] that has been derived for cases of small deflections. In this approximate solution, the deflection is found to be inversely proportional to a distance variable. We consider that such an approximation is adequate for us to investigate the contribution of gravitational deflection to redshift.

Space should not be modelled simply as an isotropic and homogeneous medium, as has quite often been suggested. Photos taken from the James Webb Space Telescope (JWST) in its deep space probes [5] have shown clusters of galaxies in certain regions, while there are huge empty spaces elsewhere. Along a given light path, a wave will experience different conditions as compared with other paths. The aim of our investigation is to find out whether, with pulse energy changes in some sections and gravitational deflections in others, the overall redshift could still be predicted by the wave propagation theory using overall averaged system parameters. Our interest is in the gradient of the wavelength versus distance plot. But our findings are in dimensionless format; we need calibration to convert them into physical entities.

In Section 2 of this paper, we describe how the NSE with an external source or with a CW background could be solved numerically. In Section 3, we describe how we calculate the deflection of a stable soliton using the approximate solution of General Relativity Theory. In Section 4, we give numerical examples that provide us with sufficient data for Discussion in Section 5. Although the propagation of solitons is governed by the local conditions that could have varying effects on the propagating wave, those effects are cumulated at each step and are carried over to the next. It is the overall redshift that is important. This redshift is observed by astronomers in their empirical Hubble law and predicted by astrophysicists in models such as the Standard Model of cosmology. But based on our numerical solutions, we conclude that the electromagnetic wave theory could be used to account for those localized transmission variations investigated.

2. Stable periodic (SP) bright solitons

The NLS equation for electromagnetic wave (soliton) propagation in dimensionless form is

$$u_x - \frac{i}{2}D(x)u_{tt} - i|u|^2u = S(x) \tag{1}$$

where u is the slowly varying envelope of the axial electric field, and $D(x)$, x, t, and S are the dispersion coefficient, the spatial propagation distance, temporal local time, and external source, respectively. The last term on the left-hand side of Eq. (1) represents self-phase modulation but without a specific system parameter.

To include a CW background, u_o into Eq. (1), let

$$u = v + u_o$$

With S = 0, substituting the above into Eq. (1) gives

$$v_x - \frac{i}{2}D(x)v_{tt} - i|v + u_o|^2(v + u_o) = 0 \tag{1a}$$

Using the same numerical procedures as described in our previous papers [1][2][3], Eq. (1) could be solved to give a stable periodic solution along the propagation distance x. The procedures involve the division of the numerical spatial time window of length L into N equal segments. Over each segment, the solution is to be approximated by an economized $(M-1)^{th}$ order power series,

$$u(t,x) = \sum_{k=1}^{M} u_k(x)t^{k-1} \tag{2}$$

Eq. (1) is discretised in the t-direction by using collocation points chosen to be the roots of a Chebychev function,

$$t_k = -\cos\left[\frac{(2k-1)\pi}{2(M-1)}\right], \quad k = 1, \ldots, M-1 \tag{3}$$

Together with the boundary conditions and all the interfacial continuity conditions between any two subdivisions, the set of ordinary differential equations so obtained is in the form,

$$AV_x(x) - iLV(x) = iQ(x,V) \tag{4}$$

where $\boldsymbol{V}$ is a [M x N] vector consisting of the coefficients of the power series used, and $\boldsymbol{A}$, $\boldsymbol{L}$, and $\boldsymbol{Q}$ are matrix

operators. As Eq. (4) is nonlinear, it could be solved by an implicit difference algorithm together with iteration.

For a bright soliton solution, a suitable initial input pulse could be,

$$u(t,0) = \beta \exp\left[-\alpha(t-0.5L)^2\right] \tag{5}$$

where *L* is the length of a given numerical window for *t*, αan arbitrarily chosen constant, and β an adjusting parameter to give a specified pulse energy, *E*,

$$E(x) = \int_{-\frac{L}{2}}^{\frac{L}{2}} \left(|u(t,x)|^2\right) dt \tag{6}$$

It is important to set the boundary conditions as

$$u(t,x) = 1000\frac{\partial u}{\partial t} - u(t,x) \quad at\ x = \pm 0.5L \tag{7}$$

The large constant associated with the derivative term will force *u* to assume a near-zero value with zero gradient so that reflection at the boundaries is minimized.

For the stable periodic solution, we integrate Eq. (4) to a total distance *Z*, with the specified dispersion coefficient − *D* for the first half and *D* for the second half of Z. We use the fact that, for an SP solution propagating through a dispersion map, the input pulse should be similar in shape to the output pulse. To reach this goal, an iterative scheme based on successive halves could be used,

$$u_{in}^{i+1} = 0.5\left(u_{\text{in}}^{i} + u_{\text{out}}^{i}\right) \tag{8}$$

where u_{in}, and u_{out} are the input and output pulses to the dispersion map, respectively, and the superscript *i* denotes the iteration number. It should be noted that SP solitons are special cases of exactly periodic solitons. But, with an exactly periodic soliton, the input pulse is exactly the same as the output pulse.

The stable periodic solitons so found could be used as the initial input to start a propagation history through sections that have various system parameters. It should be noted that for those histories, the same set of algebraic equations is used with the exception that the steps described in Eq. (8) are not included.

3. Gravitational Deflection

Based on the approximate solution [4] of the General Relativity theory, the light path deflection angle, $\Delta\Theta$, is found to be inversely proportional to the distance between the light path and the centre of the mass:

$$\Delta\Theta = \frac{4GM}{\Delta} \tag{9}$$

where *G* is the gravitational constant, *M* is the mass, and Δ is the distance between the wave front and the centre of the mass. Eq. (9) could be used in its dimensionless form,

$$\Delta\Theta = \frac{c}{\varepsilon} \tag{10}$$

where $E = \frac{C\Delta}{4GM}$. We can study the contribution of gravitational deflection by tracking the history using a single arbitrarily chosen parameter *C*. Numerically, we shall use a new rectangular coordinate system *(x1, x2).* Tracking the wavefront at a particular step, let the mass be at $((x1)_m, (x2)_m)$ and the wavefront be at $((x1)_1, (x2)_2)$; the straight line connecting the wavefront to the centre of the mass is

$$\varepsilon = \sqrt{((x1)_m - (x1)_1)^2 + ((x2)_m + (x2)_1)^2} \tag{11}$$

Then, Eq. (10) can be used to find the deflection angle $\Delta\Theta$. If a wavefront has propagated along a light path making an angle Θ with the *x1*-axis and reached $((x1)_1, (x2)_2)$, the path direction for the next integration step would be along the deflected angle, $\Theta + \Delta\Theta$. With the path integration step being Δx, the change in the wavefront position would be $\Delta x\ cos\ (\Theta + \Delta\Theta)$ and $\Delta x\ sin\ (\Theta + \Delta\Theta)$ in the *x1*- and *x2*- coordinates, respectively. Knowing the new position, Eqs. (11) and (10) could be used to find ε and $\Delta\Theta$, respectively, for the next integration step.

4. Numerical Examples

For every case in our present investigations, we start with a stable bright solution obtained numerically as described in our previous paper [3]. Using *L* = 40, *N* = 10, *M* = 20, Δx = 0.0005, *D* = - 0.1, *E* = 0.25, and a dispersion map Z = 6, Figure 1 shows that such a soliton propagates stably with an increasing wavelength. Furthermore, the same characteristics are observed when it is propagating through a section with a set of different system parameters. We retain the description of periodic because the histories are all repeatable.

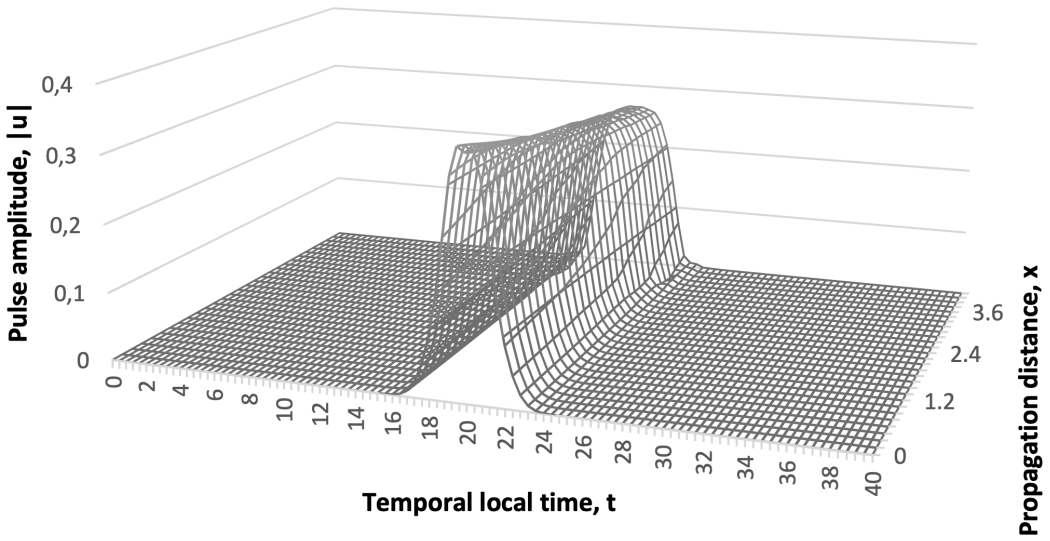

Figure 1. Propagation of bright stable periodic solution

4.1. Propagation of a bright soliton with CW background

Example 1 - Four cases (See Table 1 for details), with or without a CW background, were used to show the differences in the pulse half-width, *W*, propagation histories. (*W* is the same as FWHA, full width at half maximum, a commonly used measure for pulse width.):

doi.org/10.32388/XFMF84.2

	Propagation distance, x	Dispersion coefficient, D	CW background, u_o
Case 1	0 to 6	-0.2	0
Case 2	0 to 2	-0.2	0
	2 to 2.5	-0.2	-0.2
	2.5 to 3.5	-0.2	0
	3.5 to 4	-0.2	-0.2
	4 to 6	-0.2	0
Case 3	0 to 6	-0.1	0
Case 4	0 to 2	-0.1	0
	2 to 2.5	-0.1	0.5
	2.5 to 3.5	-0.1	0
	3.5 to 4	-0.1	0.5
	4 to 6	-0.1	0

Table 1. System parameters used in Example 1

The pulse width histories found are shown in Fig. 2. The noticeable features are: (i) the gradient is slightly higher for negative u_0, and slightly lower for positive u_0; (ii) the gradient in the sections before and after a section with a CW background remains the same.

doi.org/10.32388/XFMF84.2

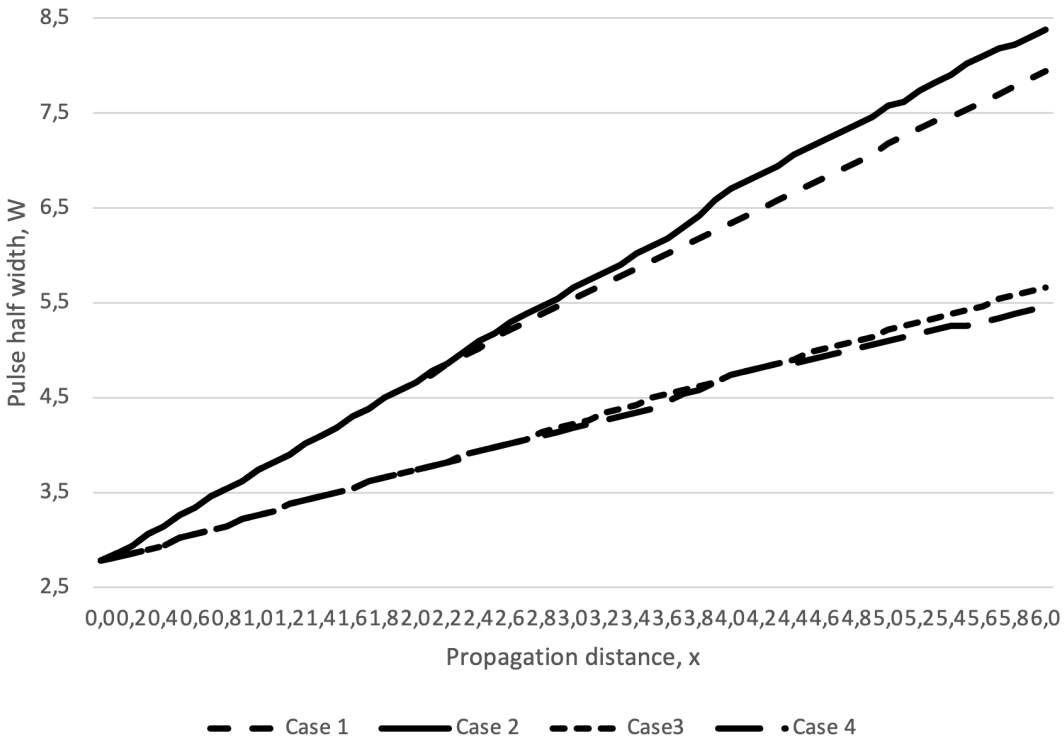

Figure 2. Effects of CW background on the half pulse width histories

Example 2 - Case 5 (See Table 2 for details) is designed to include two sections, in each, both D and u_0 have the same values but of opposite sign. In five other sections involved, the dispersion coefficient is randomly selected, but for the whole length, the overall distance-weighted average is 0.1, which is the same as Case 3 in Example 1.

doi.org/10.32388/XFMF84.2

Section	Propagation distance, x	Dispersion coefficient, D	External source, u_o
1	2	-0.2	0
2	0.5	0.2	-0.2
3	1	0.1	0
4	0.5	-0.2	0.2
5	2	-0.15	0

Table 2. System parameters for Case 5

The solutions are shown in Fig. 3, where we can see that in Sections 2 and 4, there are large decreases and increases in pulse energy due to the presence of $u_{0.}$ But the gradient change between Sections 2 and 3 is very small. The same happens between Sections 4 and 5. Also shown is the fact that the overall half pulse width change could be accurately predicted by using the average distance-weighted D as in Case 4 of Example 1.

doi.org/10.32388/XFMF84.2

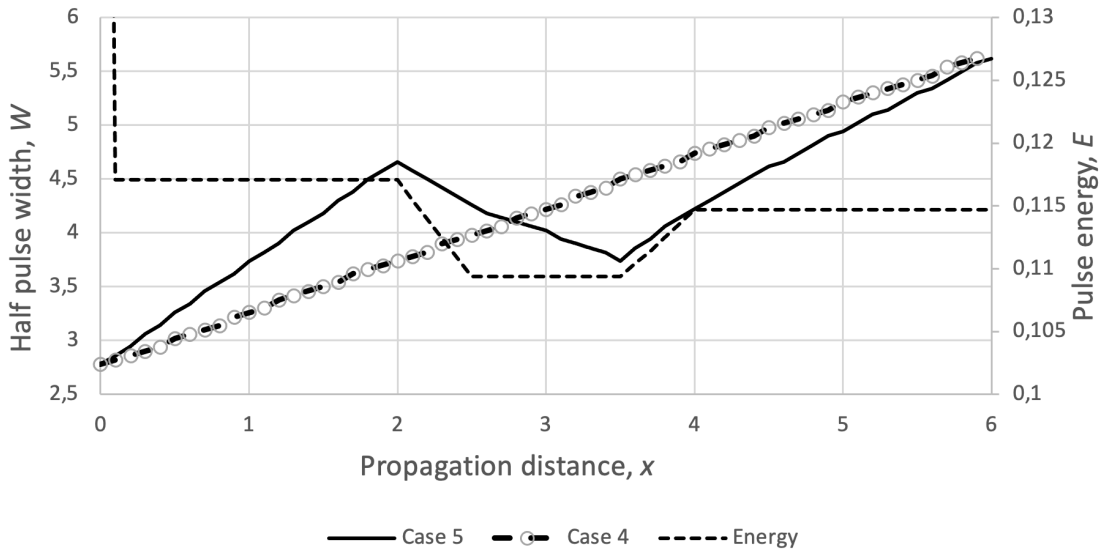

Figure 3. Histories, Cases 4 and 5, of half pulse width and pulse energy histories

4.2. Propagation of solitons with external source

Example 3 – This example, Case 6, consists of three sections that all have $D = -0.2$ but $S(x) = s\,u$, where s = 0.5, - 0.5, and 0.5, respectively, in each section. Features of the solution histories are: (i) pulse energy increases or decreases steadily according to the sign of s, and (ii) there is very little change in the wavelength half-width gradient in all sections, as can be seen in Figure 4.

4.3. Propagation with gravitational deflection

With small deflection, the propagation of electromagnetic waves is still governed by Eq. 1. The propagation distance, x, is taken to be along the deflected light path. When integrating Eq. (1) by a stepwise procedure, the deflection and tracking of the wavefront are carried out based on procedures described in Section 3.

Example 4 – Using the $x1$-, and $x2$- coordinates, the starting position is chosen to be at $(0, 0)$ with the mass located along the straight line $x1 = 0.5\,Z$, where Z is the length of the propagation distance to be investigated. If the line joining the wavefront to the centre of the mass makes an angle, φ, with the $x1$-axis, the mass is located at $(0.5\,Z, b)$, where $b = 0.5\,Z\,\tan(\varphi)$. For this example, the initial $\varphi = 20^0$, $\Theta = 0$, $Z = 3$, and $D = -0.2$. For the arbitrarily chosen constant in Eq. (10), $C = 0.00005$ and 0.0001, respectively, for Cases 7 and 8. The solutions are plotted out in Figure 5. The deflection rate (as seen in the direction changes) is the largest at $x1 = 0.5\,Z$, where the wavefront is closest to the mass. Also, a larger C gives larger deflection, as expected. Without deflection, the wavefront will move along the $x1$-axis and travel 3 units in that direction. With deflection, the wavefront has travelled the same distance along its path, the same as in the case without deflection, but shorter in terms of the $x1$-coordinate. It should be pointed out that the scaled-down dimensionless length units, $x1$ and $x2$, used here are based on the local conditions and would be many orders smaller than x, the propagation distance used in NSE, which is in billions of light years.

5. Discussion

Since the discovery of a statistically significant difference in the Hubble constant predicted by the Big Bang theory-based method and by empirical correlation, this 'Hubble tension' has not yet been resolved. A 2023 review [6] has referenced 531 papers; each has offered one or another scientific solution. But some people would insist on the Big Bang approach, often on philosophical belief, while others accept what they consider more authoritative. Scientists would ask for new evidence, such as in the call for new physics [4] [6]. Although the physics used in the Schrödinger equation is not new, it has been widely used, both in theory and in practice, for wave propagation in many

doi.org/10.32388/XFMF84.2

diverse fields. However, its application to electromagnetic waves propagating through space is a new suggestion.

There are more than 43 known mechanisms for wavelength changes [7]. Most of these mechanisms are localized effects that would not contribute significantly to the overall wavelength changes that are the central issue of Hubble tension. However, if a localized effect is recursive (happening in many sections of the light path), the contribution of this type of effect needs to be investigated. We have selected pulse energy change and *CW* background; both are recursive.

In addition to Hubble tension, another challenge facing Big Bang theory is the fact that a homogeneous and isotropic universe is assumed on a large-scale model and the cosmological principle such that one single Hubble law is supposed to cover all cases no matter how far away they are being observed. But, even on such a scale, the universe is found to be both anisotropic and inhomogeneous [8][9]. Based on what we have found numerically, the wave propagation theory need not rely on the Cosmological principle, although a set of distance-averaged parameters could be used to predict the overall wavelength shift. This is due to the fact that the waves are found to be stable, periodical, and have other innate characteristics of their propagation.

In our numerical investigations of Examples 1 and 2, we have dealt with cases where the pulse amplitude has changed gradually together with a small change in the pulse shape due to the presence of a CW background. In these cases, as can be seen in Fig. 2, our numerical predictions have indicated a small change in the gradient in the redshift–distance plot. But the changes could be cancelled out in the presence of sources of opposite sign, as in Case 5 of Example 2 and shown in Fig. 3. Also, the overall wavelength changes can be predicted by using the distance-weighted *D* without a CW background.

Pulse energy changes due to an external source proportional to the pulse itself will only affect the amplitude and not the pulse shape, as in Example 3. In these cases, there is no change in the gradient, as can be seen in Fig. 4. This is consistent with what we have found previously that pulse energy has not been an important variable in the predictions of wavelength changes [10].

We did not investigate cases of large pulse distortion due to external energy sources. However, if the waves are soliton-like, it is characteristic of such propagating waves to restore to their stable shapes once those external factors no longer exist.

If our interest is the overall wavelength changes over the entire journey through space, it should be pointed out that the total contribution due to energy changes would be quite small because of the following reasons: (i) wavelength changes are accumulated throughout the entire distance travelled, which is measured in billions of light years; the total distance over which the conditions are in favour of energy exchanges could be measured only in millions of light years; (ii) as can be seen in our Examples, there are no dramatic changes in wavelength due to energy changes; (iii) wavelength changes could be positive or negative, leading to a contribution closer to zero if the total is to be taken into consideration.

The situation with gravitational deflection is different. Gravity causes the light path to curve. Without deflection, the waves are propagating in a straight line, and the distance between two points is always shorter when compared with a curved light path. In addition, contributions are accumulative over the entire propagating distance through space. Based on our propagation theory and as shown in our numerical Example 4, the wavelength changes over a given time interval are the same with or without deflection. But the apparent gradient in the wavelength change-distance relationship, however, is higher in the presence of deflection. The implication is that waves passing through densely populated regions of space would have a noticeably longer path length than those passing through sparsely populated regions. Locally, the deflection could be large; Case 8 of Example 4 shows a total deflection of nearly 60^{o} from the original light path. But masses situated at the opposite side of the path could cause negative deflection. The fact that some waves have eventually reached the observers is evidence that the net deflection need not be considered.

Historically, the deflection and lengthening of the light path due to gravity have been used to confirm the General Relativity Theory. The lengthening of the light path has also been used as the scientific argument for an expanding universe in the early days of the Big Bang theory. Although we do not have the actual physical data, in principle, our numerical example is sufficient to demonstrate that the light path can be lengthened by gravity. But, if we accept the prediction by the General Relativity Theory, this should be the same anywhere in the universe and is not related to the position of the observer. We cannot accept the proposition in the Big Bang theory that the rate of wavelength lengthening is proportional to the distance between the light source and observers.

6. Conclusion

1. Due to the innate nature of solitons, and the balancing of the dispersion term with the nonlinear terms in NSE, electromagnetic waves can propagate stably over a long distance with wavelength changes linearly proportional to the distance travelled, although the rate of change is governed by the local prevalent conditions.
2. Solitons have both wave-like and particle-like transmission characteristics. Due to the latter characteristic, any changes are accumulated throughout the entire distance travelled.
3. Since all wavelength changes vary linearly with distance, the distance-weighted averages can be used to predict the overall shift that retains the linear relationship over any length of transmission.
4. Consideration of an inhomogeneous and anisotropic space is needed if localized events are involved. But overall contributions to redshifts observed in starlight are most likely insignificant except for gravitational deflection.

Other References

- L. Lerner, A simple calculation of the deflection of light in a Schwarzschild gravitational field, Am. J. Phys. 65 (1997) 1194-1196 https://doi.org/10.1119/1.18757

References

1. a, b, cP. Y. P. Chen, *A mathematical model for redshift, Appl. Math. 11 (2020) 146-156. https://doi: 10.4236/am.2020.113013*
2. a, b, cP. Y. P. Chen, *Propagation of dispersion-managed dark solitons and the novel application to redshift in starlight, Optik 251 (2022), 168384. https://doi.org/10.1016/j.ijleo.2021.168384*
3. a, b, c, dP. Y. P. Chen, *Investigation of nonlinear Schrödinger equation for application to astronomical Redshift, Optik 261 (2022), 169181 https://doi.org/10.1016/j.ijleo.2022.169181*
4. a, b, c, dE. D. Valentino, et al., *(2020) Cosmology Intertwined II: The Hubble Constant Tension, arXiv:2008.11284v4[Astro-ph.CO].*
5. ^C. Williams, S.Tacchella, and M. Maseda, *Webb Shows Areas of New Star Formation and Galactic Evolution James Webb Space Telescope Science. Edited by Matthew Brown, National Aeronautics and Space Administration, April 12, 2023.*
6. a, bJ. P. Hu, and F. Y.Wang, *Hubble Tension: The Evidence of New Physics, Universe, 9 (2023) 94. https://doi.org/10.3390/universe9020094*
7. ^L. Marmet, *On the interpretation of spectral red-shift in astrophysics: A survey of red-shift mechanisms – II. (2018) arXiv:1801.07582v1 [astro-ph.CO].*
8. ^K. Migkas, et al., *Probing cosmic isotropy with a new X-ray galaxy cluster sample through the LX-T scaling relation, Astronomy Astrophysics. 636 (2020):42. doi:10.1051/0004-6361/201936602*
9. ^Y. Jaswant, J. S. Bagla, and Khandai *(25 Fractal dimension as a measure of the scale of homogeneity". Monthly Notices of the Royal Astronomical Society. 405 (2009–2015). doi:10.1111/j.1365-2966.2010.*
10. ^P. Y. P. Chen, *Computational Characterization of Cosmic Redshift Based on Electromagnetic Wave Propagation Theory. Available at SSRN: https://ssrn.com/abstract=4295878 or http://dx.doi.org/10.2139/ssrn.4295878*

Declarations

Funding: No specific funding was received for this work.
Potential competing interests: No potential competing interests to declare.